PROCEEDINGS OF THE

25TH INTERNATIONAL LASER RADAR CONFERENCE

St.-Petersburg
5–9 July 2010

Volume II

Proceedings of the 25th International Laser Radar Conference, 5–9 July 2010, St.-Petersburg, Russia [Electronic source]. — Electr. data — Tomsk: Publishing House of IAO SB RAS, 2010. — CD-ROM. — PC Pentium 1 or higher; Microsoft Windows; CD-ROM 16-x and higher; mouse.

ISBN 978-5-94458-109-9

ON THE LIDAR RATIO ESTIMATION FROM THE SYNERGY BETWEEN AERONET SUN-PHOTOMETER DATA AND ELASTIC LIDAR INVERSION

M. Nadzri Md. Reba, Francesc Rocadenbosch, Michaël Sicard, Dhiraj Kumar, Sergio Tomás

Dep. of Signal Theory and Communications, Remote Sensing Lab. (RSLAB), Universitat Politècnica de Catalunya (UPC)/IEEE-CRAE. C/ Jordi Girona, 1-3, Bldg. D4-016, 08034 Barcelona, Spain; E-mail: roca@tsc.upc.edu

ABSTRACT

The method of aerosol lidar ratio estimation from combined backscatter lidar/sun photometer measurements is analytically reformulated in terms of an objective function ready to be automated by standard numerical tools. Lidar aerosol optical thickness (AOT) extrapolation methods in the lowermost part of the boundary layer where lidar data is usually no longer valid are also presented. Finally, a 532-nm case example compares the estimated lidar ratio with that from a 532/607-nm elastic/Raman lidar.

1. INTRODUCTION

Co-located co-ordinated sun-photometer measurements are becoming an essential complement to ground- and satellite-based lidars [1] and a major strategic objective of GALION [2]. Thus, while sun-photometers provide wavelength-dependent column-integrated information on the atmospheric AOT and scattering phase function, atmospheric lidars provide range-resolved information on the atmospheric aerosol layering, therefore, helping to separate AOT contributions from the boundary layer and the free troposphere.

In the standard and simplest combination of a single-wavelength backscatter lidar (BL) and a sun-photometer (SP), which is the configuration revisited in here, the two-component elastic lidar inversion algorithm (also known as Fernald's [3] or Klett-Fernald-Sasano's method, -KFS for short in what follows-) is used to derive the aerosol extinction given a point calibration in a reference range and a range-independent lidar-ratio estimate. From the inverted extinction, the lidar AOT is computed and compared with the sun-photometer measured AOT in order to estimate a *range-independent* lidar ratio [4]. This is called the "constrained" KFS algorithm.

More advanced configurations such as the combination of multi-wavelength Raman lidar with a sun-photometer enable to determine aerosol microphysical properties separately in the boundary layer and the free troposphere [5].

Sect. 2 presents the BL-SP algorithm formulation in terms of an objective function. Sect. 3 discusses a case example with Raman lidar inversion. Conclusion remarks are given in Sect. 4.

2. INVERSION METHOD

2.1 AOT from the KFS elastic inversion algorithm

The backward lidar equation solution from the KFS algorithm [3] is presented in detail in companion paper [6] and can be summarized in kernel form as

$$\beta_{aer}(S_{aer}, R_c, R) = f\left[P(R), \beta_{mol}(R), S_{aer}, R_c, R\right], \quad (1)$$

Where notation $\beta_{aer}(S_{aer}, R_c, R)$ indicates that the inverted aerosol backscatter *primarily* depends on the *user-selected* calibration point, R_c, *user-selected* lidar ratio (to be solved), S_{aer}, and range, R. Implicitly, β_{aer} also depends on the return power, $P(R)$, and the assumed atmospheric molecular profile, β_{mol}.

From the lidar-ratio definition, the aerosol extinction is

$$\alpha_{aer}(S_{aer}, R_c, R) = S_{aer}\beta(S_{aer}, R_c, R). \quad (2)$$

At this point, note that stand-alone backscatter lidars (equivalently, the "unconstrained" KFS inversion) cannot trustworthy retrieve the aerosol extinction for it is obtained by multiplying the aerosol backscatter profile by the unknown lidar ratio.

Let us call the range-independent lidar ratio, x, and let us reformulate Eq.(2) above in vector form as

$$\alpha_{aer}(S_{aer}, R_c, R) \rightarrow \vec{\alpha}_{aer}(x). \quad (3)$$

Therefore, the *lidar AOT* from height h_1 to h_2 as a function of the unknown lidar ratio x becomes

$$AOT_I(x) = \int_{h_1}^{h_2} \alpha_{aer}(x, z)dz, \qquad I = [h_1, h_2]. \quad (4)$$

2.2 Lidar AOT relative-altitude correction

In theory and in order to compare the lidar AOT of Eq.(4) above with that from the sun-photometer, AOT^{SP}, the atmospheric measurement column of both instruments must be the same. In practice, h_2 is chosen to be a conservative height, $h_2 = h_{AER}$, ensuring that there are no aerosols above. This usually yields h_2 in the free-troposphere or in the stratosphere (volcanic aerosols). h_1 corresponds to the initial measurement height of the sun-photometer column, $h_1 = h_{ASL}^{SP}$ (Fig.

1). This poses two different cases depending on the relative initial measurement heights of both instruments, h_{ASL}^{SP} for the sun-photometer, and h_{OVF} for the lidar (e.g., the height of full overlap in a biaxial system). Therefore, the lidar AOT is computed as

$$AOT(x) = \underbrace{0}_{AOT_1} + \underbrace{\int_{h_{ASL}^{SP}}^{h_{AER}} \alpha_{aer}(x,z)dz}_{AOT_2}, \qquad h_{ASL}^{SP} > h_{OVF}$$

$$AOT(x) = \underbrace{\int_{h_{ASL}^{SP}}^{h_{OVF}} \alpha_{aer}(x,z)dz}_{AOT_1} + \underbrace{\int_{h_{OVF}}^{h_{AER}} \alpha_{aer}(x,z)dz}_{AOT_2}, \qquad h_{ASL}^{SP} \le h_{OVF} \tag{5}$$

where AOT_2 is the lidar AOT contribution from the KFS-inverted extinction (height interval $I = (h_{ASL}^{SP}, h_{AER})$ in Fig. 1a, $I = (h_{OVF}, h_{AER})$ in Fig. 1b) while AOT_1 is the AOT contribution to be estimated for it is out of the lidar valid-measurement range ($I = (h_{ASL}^{SP}, h_{OVF})$ in Fig. 1b). Under a zeroth-order (i.e., flat) extrapolation, the AOT_1 can be computed from the extinction in the valid-measurement range as

$$AOT_1(x) \approx \int_{h_{ASL}^{SP}}^{h_{OVF}} \hat{\alpha}_{aer}(x,z)dz \approx \alpha_{aer}(x, h_{OVF})\left(h_{OVF} - h_{ASL}^{SP}\right). \tag{6}$$

This is a good approximation for a boundary layer homogeneously mixed from the ground (Fig. 3).

2.3 Objective function

By defining the AOT closure condition as

$$f(x) = AOT^{SP} - AOT(x), \tag{7}$$

the root of Eq.(7) yields the sought-after lidar ratio $x = S_{aer}$ (Fig. 2). Numerical inputs are the initial search interval for the lidar ratio, $[S_{aer}^{\min}, S_{aer}^{\max}]$, the sun-photometer AOT reference, AOT^{SP}, and the lidar-ratio termination error goal, $\varepsilon = \left|S_{aer} - \hat{S}_{aer}\right|$.

3. CASE EXAMPLE

To verify the method, the lidar-ratio estimate from Eq.(7) is compared with the maximum-likelihood [7] (ML) lidar ratio using the UPC 532/607-nm elastic/Raman lidar. UPC Barcelona lidar station is located 41.39ºN 2.11ºE, 115-m ASL altitude. The lidar full-overlap altitude is $h_{OVF} = 500\,m$ ASL and the line-of sight is 51-deg elevated. Barcelona AERONET sun-photometer station is located 600 m apart, at an altitude of 125-m ASL, see Tab. 1. The AOT at 440-nm wavelength as well as the 440-675-nm Ångström exponent are the major AERONET 2.0-level data used to interpolate the lidar AOT at the 532-nm laser wavelength.

Fig. 4 shows a diurnal regular lidar measurement on 29AUG2008 at 1923 UTC during a dust event episode along with back-trajectory and dust-load information. The iterative lidar-ratio search algorithm is based on a simple bisection method applied to the objective function of Eq. (7) using the AERONET measurement on 30AUG2008 at 0623UTC as the reference AOT^{SP}. A flat extrapolation (Fig. 3) is used to estimate the extinction below the lidar height of full overlap. This assumes stable and minimum variation of atmospheric conditions during the whole night. Good agreement (Fig. 4a) results between the KFS-inverted aerosol extinction, backscatter, and lidar ratio ($\hat{S}_{aer} = 54.4 \pm 1\,sr$) and those from the Raman lidar method [8] (ML estimate of $\hat{S}'_{aer} = 50 \pm 0.5\,sr$). The fact that $\hat{S}_{aer}$ and $\hat{S}'_{aer}$ error intervals do not overlap is due to the hypothesis of a range-independent lidar ratio (aerosol size distribution and composition invariant with range) [4] and the fact that the Raman-inverted extinction errorbars only assume statistical observation noise. In contrast, poor agreement results if the last AERONET AOT value on 29AUG2008 at 1717UTC is considered. This is due to large variations in the atmospheric conditions ($\hat{S}_{aer} = 79.1 \pm 1\,sr$). Fig. 3 and Tab. 2 compare higher order AOT extrapolations, orders 1-2 corresponding to not-well mixed conditions.

4. CONCLUSIONS

The well-known method of range-independent lidar ratio estimation by constraining the elastic lidar inversion algorithm with the sun-photometer AOT has been re-formulated in Fig. 2 block diagram and Eqs.(5)-(7) providing: 1) an objective function apt to be solved by any conventional root-solver algorithm and 2) inclusion of the AOT relative-altitude correction between both instruments. The proposed formulation has successfully been compared against independent Raman lidar measurements.

ACKNOWLEDGMENTS

European Commission under the EARLINET-ASOS contract nº RICA-025991 and nº 011863 (RIDS); European Space Agency (ESA) under the contract no. 21487/08/NL/HE, MICINN (Spanish Ministry of Science and Innovation) and FEDER funds under the project TEC2009-09106 and Complementary Action CGL2008-01330-E. Generalitat de Catalunya/AGAUR is also thanked for Mr. Md. Reba and Mr. Kumar's pre-doctoral fellowships. HYSPLIT model is provided by NOAA. DREAM model is provided by BSC (Barcelona Supercomputing Center).

REFERENCES

[1] Sinuyk A., et al., 2007: Simultaneous retrieval of aerosol and surface properties from a combination of AERONET and satellite data, *Remote Sens. Environ*, **107**, doi:10.1016/j.rse.2006.07.02, pp. 90–108.

[2] WMO GAW, 2007: Plan for the implementation of the GAW Aerosol Lidar Observation Network (GALION), WMO TD nº 1443.

[3] Fernald F. G., 1984: Analysis of Atmospheric Lidar Observations: Some Comments, *Appl. Opt.* **23**(5), pp. 652-3.

[4] Sasano Y., Browell E. V., Ismail S., 1985: Error Caused by Using a Constant Extinction/Backscattering Ratio in the Lidar Solution, *Appl. Opt.* **24**(22), pp. 3929-3932.

[5] Chaikovsky A., et al., 2004: CIMEL and multi-wavelength lidar measurements for troposphere aerosol altitude distributions investigation, long-range transfer monitoring and regional ecological problems solution: field validation of retrieval techniques*"*, *Optica Pura y Aplicada*, **37**, N3, pp. 3241-3246.

[6] Rocadenbosch, F., Reba M. N. Md., Sicard M., Kumar D., Tomás S., 2010: Lidar ratio estimation using a two-point calibration in an aerosol layer aloft, *Proc. 25th Int. Laser Radar Conference*.

[7] Barlow R. J., 1998: Maximum Likelihood, Sec. 5.3 in *Statistics. A Guide to the Use of Statistical Methods in Physical Sciences* (Wiley, Chichester, England), p. 83 and Eqs. (4.6)-(4.7).

[8] Ansmann A., et al., 1992: Independent measurement of extinction and backscatter profiles in cirrus clouds by using a combined Raman elastic-backscatter lidar, *Appl. Opt.* **31**(33), pp. 7113-7131.

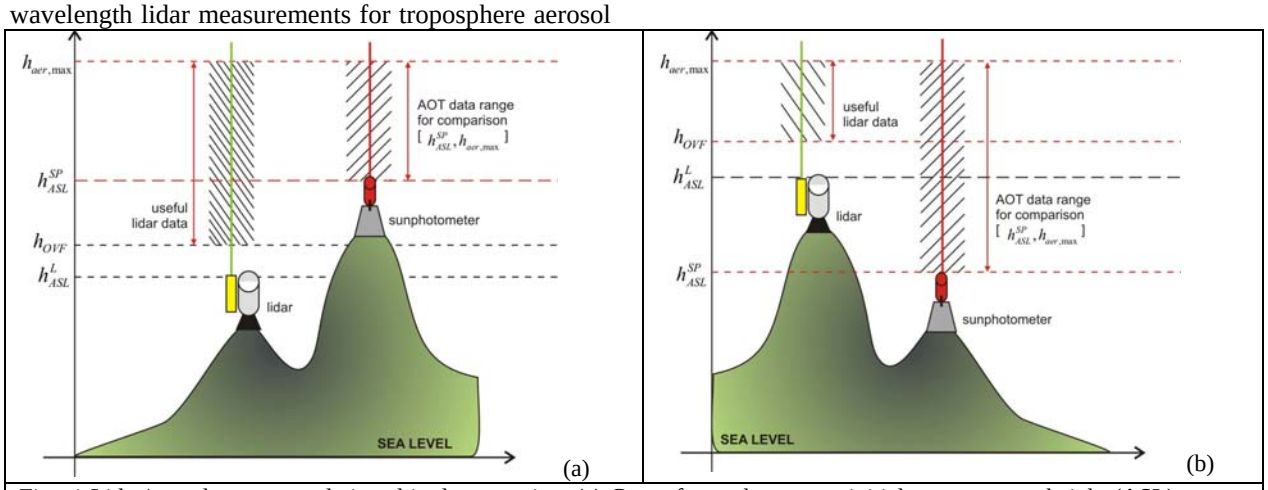

Fig. 1 Lidar/sun-photometer relative altitude correction. (a) Case of sun-photometer initial measurement height (ASL) greater than the lidar full-overlap height, $h^{SP}_{ASL} > h_{OVF}$. (b) Reverse case, $h^{SP}_{ASL} \le h_{OVF}$. Shaded height intervals indicate valid instrument data (the interval $\left(h^{L}_{ASL}, h_{OVF}\right)$ represents invalid lidar data due to e.g., incomplete overlap factor).

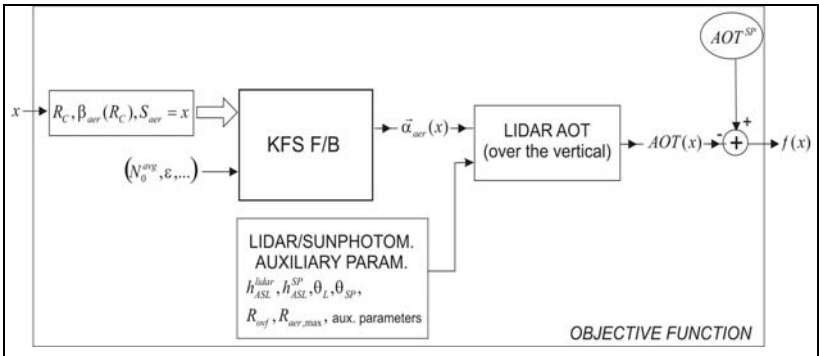

Fig. 2 Objective function block diagram to estimate the lidar ratio from combined lidar/sun-photometer measurements. $f(x)$ is the objective function (Eq. (7)), x is the lidar-ratio root estimate, AOT^{SP} is the sun-photometer AOT constraint, "KFS F/B" block represents the Klett-Fernald-Sasano inversion algorithm (Eq.(2)), and "LIDAR AOT" block implements Eq.(5).

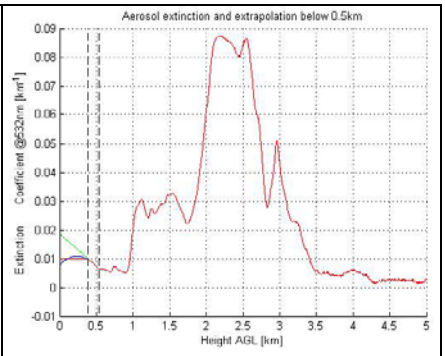

Fig. 3 Inverted aerosol extinction (case example) and extrapolation techniques below the range of full overlap: 1) Flat (red), Eq.(6), 2) Linear (blue), and 3) Quadratic (green), see Tab. 1 and Tab. 2. Vertical blue dashed lines indicate the extrapolation reference height interval.

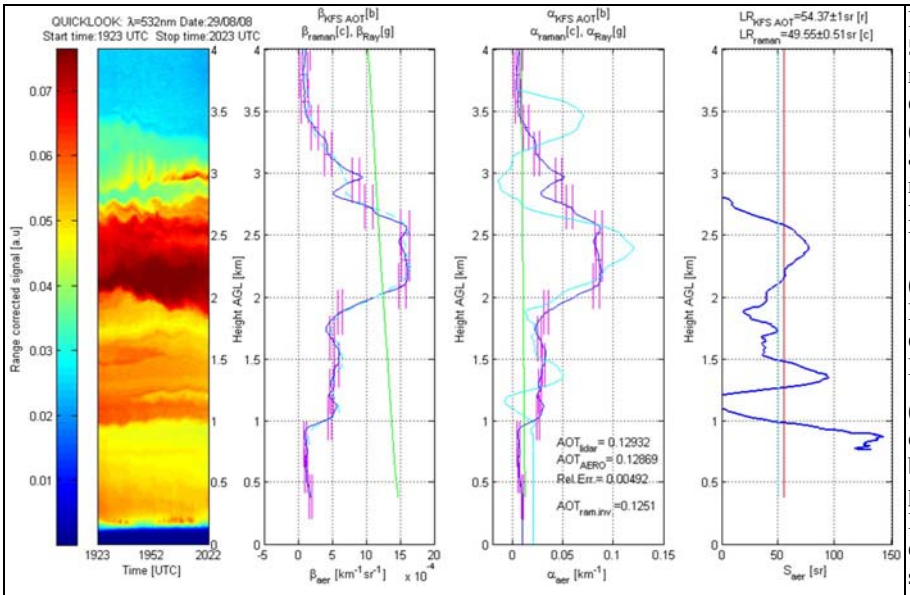

(a)

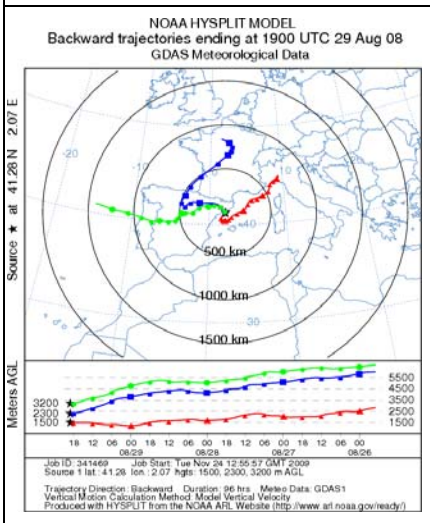

(b)

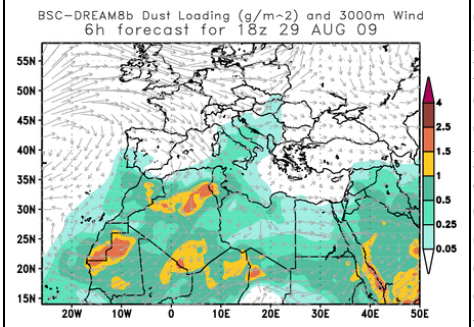

(c)

Fig. 4 Case example: Retrieval of 532-nm optical parameters and range-independent lidar-ratio estimation from combined BL-SP (backscatter lidar – sun photometer) and 532/607-nm Raman lidar measurements (Campus Nord (UPC), Barcelona, 29AUG2008, 1923-2023 UTC (dust event)).

(a) (Left to right) Range-corrected lidar signal (RCS), inverted aerosol extinction, aerosol backscatter, and lidar ratio (height is AGL).

(1st left) RCS from the 532-nm lidar channel. (2nd left) Comparison between the aerosol backscatter profile derived from the proposed BL-SP algorithm, Eq.(7) (KFS elastic inversion constrained with the sun-photometer) (solid blue, detail in Fig. 3) and from the Raman lidar algorithm [8] (dash cyan). Errorbars (magenta) indicate the 1-σ noise-induced inversion error. Rayleigh level in (green) (3rd left) Same comparison for the aerosol extinction. (4th left) Lidar-ratio profile from the Raman lidar algorithm (blue trace) and its corresponding maximum likelihood (ML) estimate [7], 50±0.5 sr (dotted cyan). The ML estimate from the combined BL-SP algorithm (Eq.(7)) yields 54.4±1 sr (red).

(b) 96-h NOAA HySplit back-trajectories ending at 1900UTC 29AUG2008.

(c) Dust-load map and synoptic wind at 3000 m ASL forecasted by DREAM on 29AUG2008, 1800UTC.

DESCRIPTION	VARIABLE	VALUE
Sun-photometer AOT	AOT^{SP}	0.129
Lidar full-overlap height, h_{OVF} . Aerosol-load maximum height, $h_{aer}^{\max}$	$\left(h_{OVF}, h_{aer}^{\max}\right)$	(0.500, 7.774) km ASL
Sun-photometer height	h_{ASL}^{SP}	0.125 km ASL
Lidar height	h_{ASL}^{L}	0.115 km ASL
Extrapolation reference height interval	$\left(h_{ext}^{\min}, h_{ext}^{\max}\right)$	(0.500, 0.730) km ASL
Lidar-ratio initial search interval	$\left(S_{aer}^{\min}, S_{aer}^{\max}\right)$	(1, 100) sr
Lidar-ratio error goal	ε	1 sr

Tab. 1 (left) Algorithm input parameters.

EXTRAPOLATION POLYNOMIAL ORDER	RESULTS	
	$\hat{S}_{aer}$	AOT_1 / AOT
0 (constant)	54.4	2.8 %
1 (linear)	52.8	3.8 %
2 (quadratic)	51.3	5.3 %

Tab. 2 (above) Lidar-ratio estimation as a function of the extrapolation technique used below the lidar height of full overlap (h_{OVF}), see Fig. 3. AOT_1 / AOT is the percentage contribution of the extrapolated extinction (AOT_1 via Eq. (6) to AOT via Eq. (5)).